

Calorimetric studies of the energy deposition on a material surface by plasma jets generated with QSPA and MPC devices

Alexander A. Chuvilo,
Igor E. Garkusha,
Vadym A. Makhraj,
Yu. V. Petrov

Abstract. Studies of the energy deposition by plasma jets incident on a material surface are of topical interest for both the fusion and plasma technology applications. In this paper the results are reported of a comparative study of plasma energy deposition on different material surfaces exposed to plasma jets of various duration and energy density, generated using the QSPA Kh-50 and the MPC devices. The spatial distribution of plasma energy density and the heat load on the surface were measured with a movable calorimeter. The measurements demonstrate that in the case of an exposure to QSPA plasma jets the absorbed heat load is approximately equal to 55–60% of the energy in the incident plasma jet. In the case of plasma jets generated using the MPC device the heat load on the target surface and was practically the same as for the QSPA jets, and additional shielding effects were found to be negligible due to the short duration of plasma jets.

Key words: quasi steady-state plasma accelerator (QSPA) • energy density • heat load • plasma streams • plasma-surface interaction

Introduction

A key feature of the plasma-surface interaction in the dense and hot plasma environment is the formation of shielding layer on the exposed surface. A comprehensive experimental study of plasma shield formation under plasma heat loads simulating disruptions in the international thermonuclear experimental research (ITER) tokamak (i.e. the heat load to the exposed surface of the order of $Q_{\text{disr}} = 10\text{--}100 \text{ MJ/m}^2$ in the time interval of 1–10 ms) was performed using the pulsed plasma gun MK-200 (Troitsk, Russia) and the quasi-stationary plasma accelerator Kh-50 (Kharkov, Ukraine) [3–5, 9]. The disruption simulation experiments had shown that due to the formation of a vapour shield on the exposed surface only few percent of the supplied energy is absorbed by the material [1]. These investigations considerably improved our understanding of the plasma-material interaction under disruptions conditions and were used for benchmarking of predictive codes [6, 7].

The energy density that could be deposited in ITER as a result of edge localized modes (ELMs) is much smaller than that for disruptions. The ELM heat loads in ITER are expected to be up to $Q < 3 \text{ MJ/m}^2$ during a time interval of 0.1–0.5 ms [8]. However, some shielding can also appear in this case. The onset of a vapour shield development and effects of the “weak” shielding for a single ELM may contribute noticeably to the resulting surface damage due to the expected large number of repetitive ELMs (up to 10^6).

A. A. Chuvilo✉, I. E. Garkusha, V. A. Makhraj,
Yu. V. Petrov
Institute of Plasma Physics,
National Science Center, Kharkov Institute of Physics
and Technology (NSC KIPT),
1 Academicheskaya Str., Kharkov, 61108, Ukraine,
Tel.: +38 057 335 6726, Fax: +38 057 335 2664,
E-mail: chuvilo@kipt.kharkov.ua

Received: 10 July 2011
Accepted: 4 January 2012

At the same time, it is known that a dense plasma cloud of heavy gases may provide an effective shielding of the divertor plates in disruption mitigation schemes due to the high emissivity of heavy gases resulting in a re-radiation of the impacting energy. In this paper we report results of an investigation of plasma-surface interaction in quasi-steady plasma states and compression plasma streams with large energy flux.

Experimental setup and diagnostics

Measurements of the plasma energy density and the surface heat load during the plasma-surface interaction were performed using the quasi steady-state plasma accelerator (QSPA) Kh-50 and the magnetoplasma compressor (MPC).

QSPA Kh-50 is the largest and the most powerful device of its kind in the world [3–5, 9]. The QSPA plasma parameters were varied both by changing the dynamics and the amount of gas filling the accelerator channel and by adjusting of the operating voltage of the capacitor bank powering the discharge. The main parameters of the QSPA plasma streams were as follows: the energy of impacting ions approximately equal to 0.4–0.6 keV, the maximum plasma pressure 3.2 bars, and the plasma jet diameter approximately equal to 18 cm. The surface energy loads measured with a calorimeter varied in the range of 0.1–1.1 MJ/m². The plasma pulse shape was approximately triangular, with the pulse duration of approximately 0.25 ms.

The MPC device consists of two copper coaxial electrodes with a disk current collector and a pulsed gas

supply system. The outer electrode consists of a 147 mm long solid cylindrical part and an output rod structure consisting of 12 copper rods, each 147 mm long. The rods form the frustum of a conical surface with an apex angle of 30°. A capacitor bank with a capacitance of 90 μ F and a maximum voltage of 25 kV was used as a power supply for the main discharge in MPC. The working pressure in the vacuum chamber was 2 torr. The plasma jet parameters were as follows: the average plasma density 10^{17} cm⁻³, the energy density $q = 0.4$ MJ/m², the plasma pulse duration 10–20 μ s, the discharge current $I_d = 500$ kA. Helium and xenon were used as working gases. Two operating modes were realized in these experiments: a pure helium discharge and a combined discharge with a local injection of xenon (7 cm³ extrapolated to the atmospheric pressure) into the compression zone. The design of the MPC device is described in detail in [2].

Measurements of the plasma stream pressure were carried out with a piezoelectric detector. The plasma stream power and the energy density were calculated on the basis of measurements of the time-dependent plasma pressure, plasma stream density and plasma velocity. An array of optical diagnostics included a diffractive spectrograph DFS-452, a monochromator MDR-23, and other compact universal monochromators, photodiodes and photomultiplier tubes. Observations of plasma interaction with the exposed surfaces were performed with a high-speed CMOS camera PCO AG. Photographs from the high-speed camera are presented in Fig. 1. Dynamics of the plasma-target interaction is shown with the frame exposition time of 1.2 ms.

The spatial distribution of the plasma energy density and the heat load on the surfaces were measured

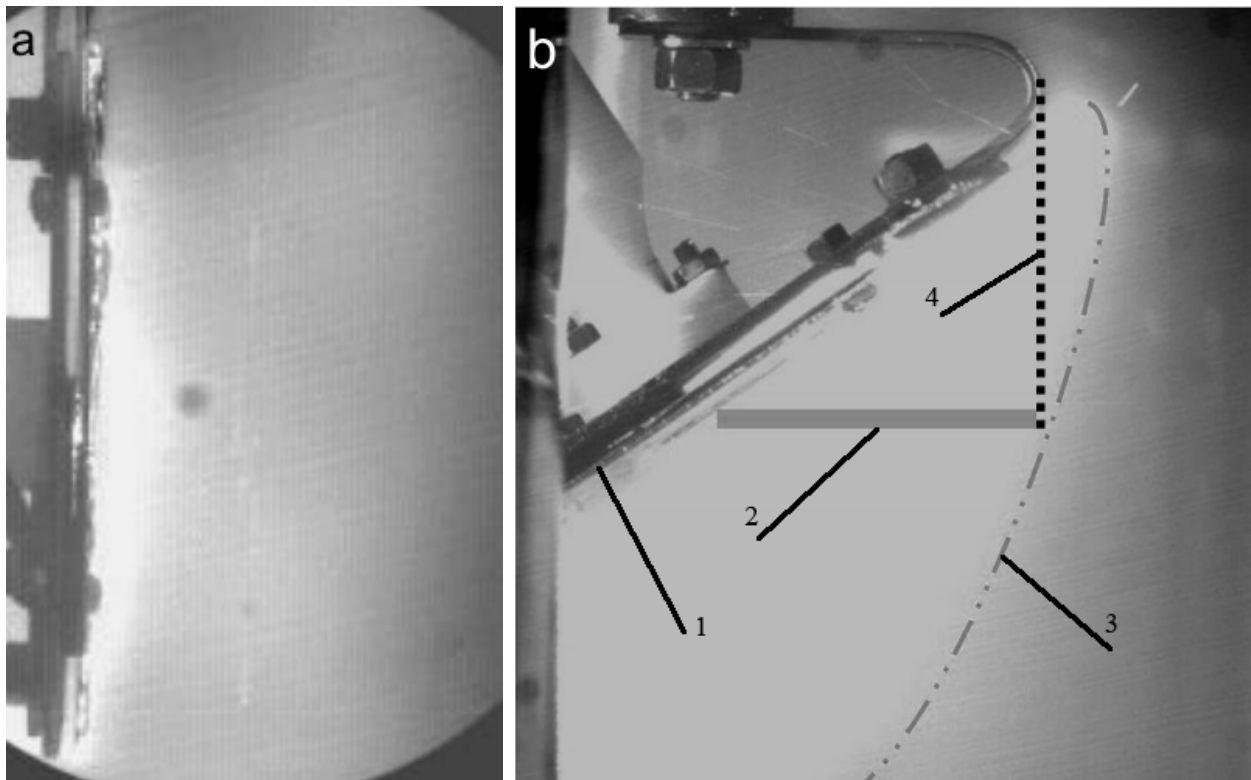


Fig. 1. Images of plasma jet interaction with the target at the time interval of 30 μ s from the beginning of the plasma-surface interaction: a normal plasma jet incidence (a) and an oblique plasma jet incidence (b). The position of the calorimeter and the location of the shielding layer are also schematically indicated. 1 – the target; 2 – the calorimeter placed at the distance of 7 cm in front of the target; 3 – the shielding layer; 4 – normal incidence.

with a movable calorimeter with a diameter of 5 mm [1]. The actual heat load on the irradiated surfaces was measured when the surface of the calorimeter and the surface of the target were in the same plane. The energy density in the shielding layer was measured by displacing the calorimeter through a hole in the center of the sample. The calorimeter could be moved into the near-surface plasma up to the distance of 5 cm from the target. In QSPA experiments the diameter of the target was 12 cm. The MPC plasma exposures were performed for 5 cm targets. A schematic diagram of the experiment for oblique impacts is shown in Fig. 1b.

Results of experiments

Energy density in free plasma streams

The spatial distribution of the energy density, measured with a calorimeter in the QSPA plasma stream at a distance of 2.3 m and 3.6 m from the accelerator is presented in Fig. 2a. The distribution of the energy density close to the axis (up to 10 cm in the radial direction) is uniform. The maximum value of the energy density in the plasma stream was found to be 2.4 MJ/m² and it decreases with increasing distance from the accelerator. This effect is due to a decrease in the plasma density with increasing distance from the accelerator. The effective diameter of the plasma stream at the target position is approximately 20 cm.

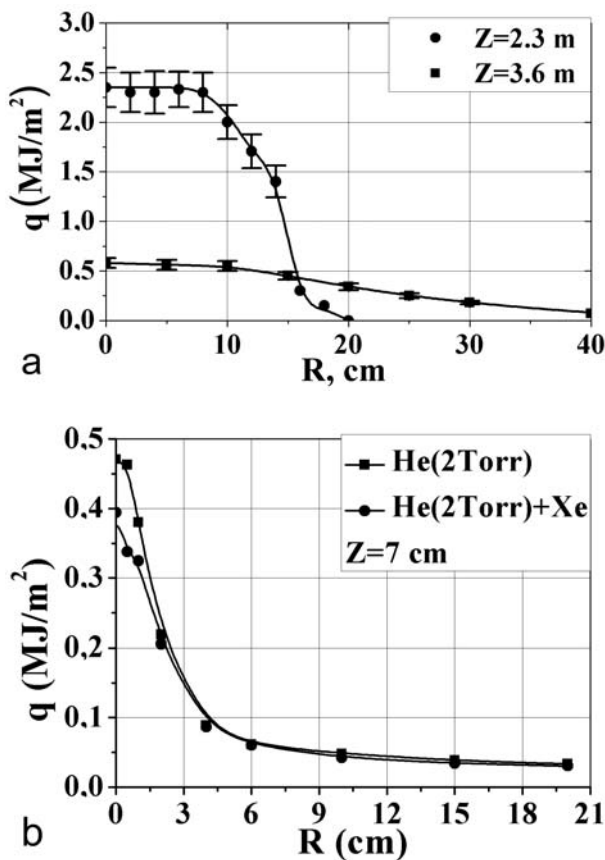


Fig. 2. Distributions of plasma jet energy density in the radial direction, measured in the case of normal plasma jet incidence, at different distances (Z) from the accelerator in the QSPA Kh-50 experiment (a) and the MPC experiment (b).

As it was shown earlier [1] for disruption-like heat loads of 25–30 MJ/m² the effect of shielding is visible even for the calorimeter of 5 mm in diameter and its readings underestimate the actual values. For this reason the energy density in the plasma stream in disruption simulation regime was determined on the basis of time resolved measurements of the plasma stream density and the plasma velocity. The value $q \approx 2.4$ MJ/m² obtained in this experiment agrees well with the theoretically calculated energy density $q \sim 2.5$ MJ/m². The total energy content was estimated by integration of the radial profiles of the energy density; this was done for several distances from the accelerator. The total energy estimated in this way is approximately equal to 150 kJ.

In the MPC plasma jets the maximum of the energy density was also found on the axis of the plasma flow, independently of the mode of operation (Fig. 2b). For a discharge in pure helium the maximum energy density obtained was 0.47 MJ/m². For discharges with additional injection of xenon the energy density did not exceed 0.39 MJ/m². The total energy deposited near the axis of the flow reached 0.41 kJ and 0.36 kJ for discharges in pure helium and in a mixture of helium and xenon, respectively. The reduction of the total deposited energy in the helium plasma with the injection of xenon is caused by energy losses for ionization of heavy impurities. For radii exceeding 2 cm the energy density in the jet is not sensitive to the presence of xenon in the plasma jet. Thus a highly localised injection of heavy gas into plasma is realised. The energy density measured at the distance of 6 cm and more from the axis does not depend on the azimuthal position of the calorimeter on the target surface. The parameters of this part of the plasma jet are only weakly sensitive to the variation of the discharge parameters.

Plasma-surface interaction

Results of the measurements of heat loads on the target surface in QSPA are presented in Fig. 3. The heat load on the target surface was found to increase with the increasing energy density in the incident plasma jet. The energy density absorbed by the target surfaces is only about 50–60% of the QSPA plasma energy density $q \geq 0.5$ MJ/m². This reduction in the energy density is caused by the formation of a dense shielding layer protecting the target surface. The shielding layer is formed during the first microsecond of the plasma-surface interaction. The plasma density in this layer can exceed the plasma density in the incident plasma jet by a factor of ten [1].

The energy density increases with an increasing distance from the target surface (Fig. 3). For the normal incidence, the energy density saturates at some distance from the surface (2–4 cm, depending on the energy density in the plasma jet) reaching the energy density of the incident plasma. This shows that only a part of the plasma jet energy is transferred to the target through the shielding plasma layer. The shielding layer is visible in Fig. 1a, where the bright area corresponds to the region of maximum density. A homogeneous distribution of the energy density along the target surface is observed under the normal incidence.

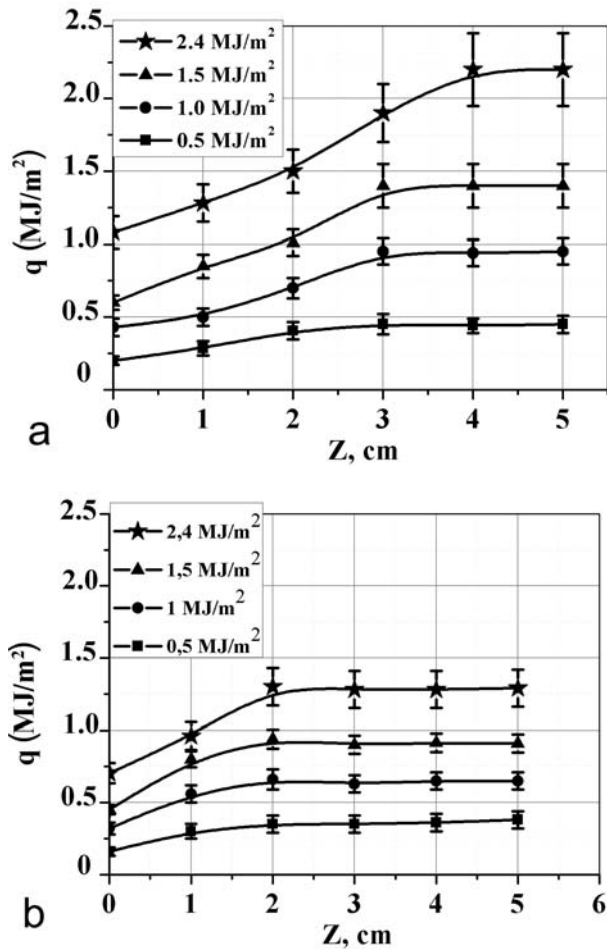


Fig. 3. The energy density distribution in the shielding layer vs. the distance from the target surface (Z) for a normal (a) and an oblique incidence (45°) (b).

Results of the energy density measurements in a shielding layer produced by plasma jets obliquely incident on the target are presented in Fig. 3b. A photograph of the shielding layer is shown in Fig. 1b. It was found that the thickness of the shielding layer was not uniform over the target surface. With the increasing incidence angle the heat load on the target surface is decreased relative to the normal impact shown in Fig. 3. The energy density is increasing with the increasing distance from the target surface in the same way as in the case of the normal incidence, but it saturates at the distance of 2 cm from the surface. Even at the greatest of the possible distances (5 cm) from the exposed surface the measured energy density is less than the energy density in the incident plasma stream. Thus a calorimeter placed in this position is still within the shielding layer.

The heat load on the surface of targets irradiated by plasma jets was also measured for jets generated with the MPC device. The target was set perpendicularly to the plasma jet. For a discharge in pure helium the heat load on target surface was measured to be 0.39 MJ/m^2 . The heat load on the tungsten surface exposed to the plasma jet with the additional injection of xenon was found to be 0.33 MJ/m^2 . This shows that the difference between the energy density in the incident plasma and the energy density delivered to target surface does not exceed 15%. This effect may be explained by the short

duration of the plasma-surface interaction (of the order of $10\text{--}20 \mu\text{s}$) and a negligible growth of shielding effects when the target diameter was increased from 5 mm to 5 cm.

Summary

Various aspects of the plasma-surface interaction were studied in a sequence of plasma jet impacts with the energy density up to 2.4 MJ/m^2 . The energy density at the surface and the heat load on the exposed surface were measured in compressive plasma jets generated with the MPC and QSPA devices.

It was found that only a part of the energy from the QSPA plasma reaches the target surface as a result of the plasma-target interaction. The energy density measured with the calorimeter in the plasma near the target surface is increasing with increasing distance from the target surface, until it reaches the energy density of the incident plasma at the distance of 3–5 cm from the surface (depending on the energy of the plasma jet). The energy density absorbed at the surface depends on the plasma incidence angle on the target. For plasma jets incident at an oblique angle it was found that the shielding layer is not uniform. The energy density is the highest for a normal incidence.

Experiments carried out with the MPC device showed that an additional injection of xenon into the compression zone leads to a decrease in the energy density in the region close to the axis. The difference between the energy density of the impacting MPC plasma and the energy absorbed by the target surface does not exceed 15%.

The plasma-surface interactions in the case of plasma jets generated by the QSPA device (with duration of 0.25 ms) were compared with the interactions obtained with short-pulse plasma jets generated using the MPC device (with duration of $10\text{--}20 \mu\text{s}$). It was shown that the exposed surface may be protected by an additional injection of a heavy gas. The results obtained in these experiments may be used to estimate the damage suffered by tungsten elements brought into contact with a hot plasma, as well as for benchmarking of the numerical codes.

References

1. Chebotarev VV, Garkusha IE, Garkusha VV *et al.* (1996) Characteristics of transient plasma layers produced by irradiation of graphite targets by high power quasi-stationary plasma streams under the disruption simulation conditions. *J Nucl Mater* 233/237:736–740
2. Chebotarev VV, Garkusha IE, Ladygina MS *et al.* (2006) Investigation of pinching discharges in MPC device operating with nitrogen and xenon gases. *Czech J Phys* 56:335–341
3. Garkusha IE, Arkhipov NI, Klimov NS *et al.* (2009) The latest results from ELM-simulation experiments in plasma accelerators. *Phys Scr* 138:014054 (6 pp), doi:10.1088/0031-8949/2009/T138/014054
4. Garkusha IE, Bandura AN, Byrka OV *et al.* (2009) Damage to preheated tungsten targets after multiple plasma impacts simulating ITER ELMs. *J Nucl Mater* 386/388:126–131

5. Garkusha IE, Bazylev BN, Bandura AN *et al.* (2007) Tungsten melt layer erosion due to $J \times B$ force under conditions relevant to ITER ELMs. *J Nucl Mater* 363/365:1021–1025
6. Landman IS, Pestchanyi SE, Igitkhanov Y, Pitts R (2010) Modeling of wall and SOL processes and contamination of ITER plasma after impurity injection with the tokamak code TOKES. *Fusion Eng Des* 85:1366–1370
7. Landman IS, Pestchanyi SE, Safronov VM, Bazylev BN, Garkusha IE (2004) Material surface damage under high pulse loads typical for ELM bursts and disruptions in ITER. *Phys Scr* 111:206–212
8. Loarte A, Saibene G, Sartori R *et al.* (2003) Characteristics of type I ELM energy and particle losses in existing devices and their extrapolation to ITER. *Plasma Phys Control Fusion* 45:1549–1569
9. Tereshin VI, Chebotarev VV, Solyakov DG *et al.* (2002) Powerful quasi-steady-state plasma accelerator for fusion experiments. *Braz J Phys* 32:165–171